

The Double Pulsar – A New Testbed for Relativistic Gravity

M. Kramer,¹ A. G. Lyne,¹ M. Burgay,² A. Possenti,^{3,4}
R. N. Manchester,⁵ F. Camilo,⁶ M. A. McLaughlin,¹ D. R. Lorimer,¹
N. D’Amico,^{4,7} B. C. Joshi,⁸ J. Reynolds,⁵, P. C. C. Freire⁹

¹*University of Manchester, Jodrell Bank Observatory, UK,* ²*Universita degli Studi di Bologna, Dipartimento di Astronomia, Italy,* ³*INAF - Osservatorio Astronomica di Bologna, Italy,* ⁴*INAF - Osservatorio Astronomica di Cagliari, Italy,* ⁵*ATNF, CSIRO, Australia,* ⁶*Columbia Astrophysics Laboratory, Columbia University, USA,* ⁷*Universita degli Studi di Cagliari, Dipartimento di Fisica, Italy,* ⁸*NCRA, Pune, India,* ⁹*NAIC, Arecibo Observatory, USA*

Abstract. The first ever double pulsar, discovered by our team a few months ago, consists of two radio pulsars, one with a period of 22 ms and the other with a period of 2.7 s. This binary system, with an orbital period of only 2.4 hours, provides a truly unique laboratory for relativistic gravitational physics. Here we summarize recently published results and we discuss the prospects of future observations.

1. Introduction

Burgay et al. (in this volume) describe the discovery of the compact double-neutron-star system PSR J0737–3039 and its implications for ground-based gravitational-wave detectors and tests of general relativity (see also Burgay et al. 2003). With the discovery of radio pulses from the companion, the system becomes unique in its potential as a testbed for relativistic gravity. The data, resulting in the timing parameters presented for both pulsars by Lyne et al. (2004) and shown here in Table 1, were obtained with the Parkes radio telescope and the Lovell telescope at Jodrell Bank. An updated timing solution covering a full year of observations will be presented in a forthcoming paper (Kramer et al., in preparation). Manchester et al. (in this volume) discuss the implications for studying pulsar magnetospheres.

2. Tests of General Relativity

As neutron stars are very compact massive objects, double-neutron-star (DNS) binaries are almost ideal sources for testing theories of gravity in the strong-gravitational-field limit. Tests can be performed when a number of relativistic corrections to the Keplerian description of the orbit, the so-called “post-

Keplerian” (PK) parameters, are measured. For point masses with negligible spin contributions, the PK parameters in each theory should only be functions of the a priori unknown neutron star masses, m_A and m_B , and the precisely measured Keplerian parameters. With the two masses as the only free parameters, the measurement of three or more PK parameters over-constrains the system, and thereby provides a test ground for theories of gravity. In a theory that describes the binary system correctly, the PK parameters produce theory-dependent lines in a mass–mass diagram that all intersect at a single point. (See Weisberg & Taylor, in this volume, for an update on the tests provided by PSR B1913+16, and Stairs, in this volume, for tests possible with PSR B1534+12.) As shown in Table 1, we have measured PSR J0737–3037A’s advance of periastron, $\dot{\omega}$, and the gravitational-redshift / time-dilation parameter γ , and we have also detected the Shapiro delay in the pulse arrival times of pulsar A due to the gravitational field of its companion (see Fig. 1), providing a precise measurement of the orbital inclination $s \equiv \sin i = 0.9995^{(+4}_{-32})$ and the “range” parameter r . This already provides four measured PK parameters, resulting in a $m_A - m_B$ plot shown in Figure 2, where we label $\dot{\omega}(m_A, m_B)$, $\gamma(m_A, m_B)$, $r(m_A, m_B)$, $s(m_A, m_B)$ as predicted by general relativity (Damour & Deruelle 1986).

In addition to these tests with PK parameters, the detection of the companion as a pulsar (B) opens up opportunities that go well beyond what is possible with previously known DNS systems. With a measurement of the projected semi-major axes of the orbits of both A and B (see Table 1), we obtain a precise measurement of the mass ratio, $R(m_A, m_B) \equiv m_A/m_B = x_B/x_A$, providing a further constraint displayed in Figure 2. For every realistic theory of gravity, we can expect the mass ratio R to follow this simple relation (Damour & Taylor 1992). Most importantly, the R -line is not only theory-independent, but also independent of strong-field (self-field) effects, in contrast to PK parameters. This provides a stringent and new constraint for tests of gravitational theories as any intersection of the PK parameters *must* be located on the R -line in Figure 2. With four PK parameters already available, this additional constraint makes PSR J0737–3039 the most overdetermined DNS system to date where the most relativistic effects can be studied in the strong-field limit.

3. Future Potential

We expect to measure the orbital period derivative, \dot{P}_b , by autumn 2004. We note that the distance to this pulsar will be needed to correctly account for relative accelerations and hence to interpret \dot{P}_b in the context of gravitational theories. VLBI observations to determine the system’s parallax are underway. In the longer term, further effects should be measurable.

3.1. Geodetic Precession and Aberration

In general relativity, the proper reference frame of a freely-falling object suffers a precession with respect to a distant observer, called geodetic precession. In a binary pulsar system this geodetic precession leads to a relativistic spin-orbit coupling, analogous to spin-orbit coupling in atomic physics (Damour & Ruffini

Table 1. Observed and derived parameters of PSR J0737–3039A and B. Standard errors are given in parentheses after the values and are in units of the least significant digit(s).

Pulsar	PSR J0737–3039A	PSR J0737–3039B
Pulse period P (ms)	22.69937855615(6)	2773.4607474(4)
Period derivative \dot{P}	$1.74(5) \times 10^{-18}$	$0.88(13) \times 10^{-15}$
Epoch of period (MJD)	52870.0	52870.0
Right ascension (J2000)	07 ^h 37 ^m 51 ^s .247(2)	–
Declination (J2000)	–30°39′40″.74(3)	–
Orbital period P_b (day)	0.102251563(1)	–
Eccentricity e	0.087779(5)	–
Epoch of periastron T_0 (MJD)	52870.0120589(6)	–
Longitude of periastron ω (deg)	73.805(3)	73.805 + 180.0
Projected semi-major axis $x = a \sin i/c$ (sec)	1.41504(2)	1.513(4)
Advance of periastron $\dot{\omega}$ (deg/yr)	16.90(1)	–
Gravitational redshift parameter γ (ms)	0.38(5)	–
Shapiro delay parameter s	0.9995(–32, +4)	–
Shapiro delay parameter r (μ s)	5.6(–12, +18)	–
Total system mass $m_A + m_B$ (M_\odot)	–	2.588(3)
Mass ratio $R \equiv m_A/m_B$	–	1.069(6)
Orbital inclination from Shapiro s (deg)	–	87(3)
Orbital inclination from $(R, \dot{\omega})$ (deg)	–	87.7(–29, +17)
Stellar mass from $(R, \dot{\omega})$ (M_\odot)	1.337(5)	1.250(5)

1974). As a consequence, the pulsar spin precesses about the total angular momentum, changing the relative orientation of the pulsar towards Earth. Since the orbital angular momentum is much larger than the pulsars’ spins, the total angular momentum is practically represented by the orbital spin. The precession rate (Barker & O’Connell 1975; Börner et al. 1975) depends on the period and the eccentricity of the orbit as well as the pulsar and companion masses. With the parameters shown in Table 1, general relativity predicts precession periods of only 75 yr for A and 71 yr for B.

Geodetic precession should have a direct effect on the timing as it causes the polar angles of the spins and hence the effects of aberration to change with time (Damour & Taylor 1992). These changes modify the *observed* orbital parameters, like projected semi-major axis and eccentricity, which differ from the *intrinsic* values by an aberration dependent term, potentially allowing us to infer the system geometry. Other consequences of geodetic precession can be expected to be detected much sooner. These arise from changes in the pulse shape and its polarisation properties due to changing cuts through the emission beam as the pulsar spin axis precesses. Due to these effects, which may complicate the TOA determination, geodetic precession is detected for PSR B1913+16 (Kramer 1998; Weisberg & Taylor, in this volume) and PSR B1534+12 (Arzoumanian 1995; Stairs, in this volume). For PSR B1913+16 it is used to derive a two-dimensional map of the emission beam (Weisberg & Taylor 2002) and to determine the full system geometry, leading to the prediction that the pulsar will no longer be observable from Earth around 2025 (Kramer 1998). Since the

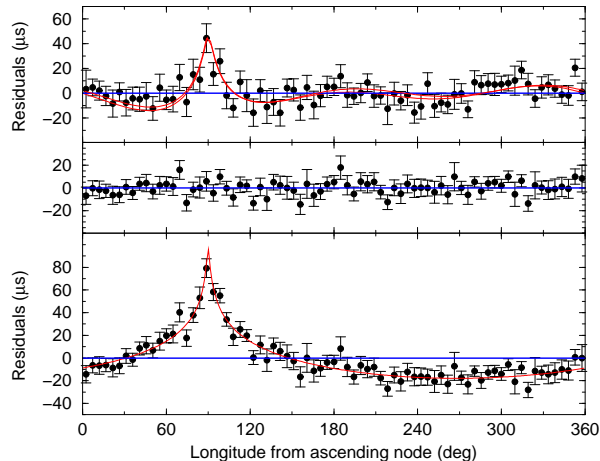


Figure 1. The effect of the Shapiro delay caused by the gravitational potential of B seen in the timing residuals of A. Residuals were averaged into 75 equal bins of orbital phase. Top: timing residuals obtained by fitting all model parameters shown in Table 1 except the Shapiro delay parameters r and s . The leftover structure represents the higher harmonics of the Shapiro delay that are unabsorbed by fits to the Roemer delay. Middle: timing residuals after fitting additionally for the Shapiro delay. Bottom: as middle panel, but with the Shapiro delay parameters r and s set to zero.

precession rates for A and B are about four times larger, the corresponding effects in PSR J0737–3039 should be much easier to detect.

3.2. Higher Post-Newtonian Orders

In all previous tests of general relativity involving PK parameters, it was sufficient to compare the observed values to theoretical expressions computed to their lowest post-Newtonian approximation. However, higher-order corrections may become important if relativistic effects are large and timing precision is sufficiently high. While this has not been the case in the past, the double pulsar system may allow measurements of these effects in the future (see Lyne et al. 2004).

Light Propagation Effects Higher-order corrections to the present description of the light propagation would account for the assumptions currently made in the computation of the Shapiro delay, that gravitational potentials are static and weak everywhere. Corresponding calculations taking these next higher-order corrections into account have been presented by Wex (1995a), Kopeikin & Schäfer (1999), and Kopeikin (2003).

In addition to light propagation effects causing time delays, others exist that are related to light bending and its consequences. Light bending as discussed by Doroshenko & Kopeikin (1995) would be superposed on the Shapiro delay as a typically much weaker signal, which arises due to a modulation of the pulsars'

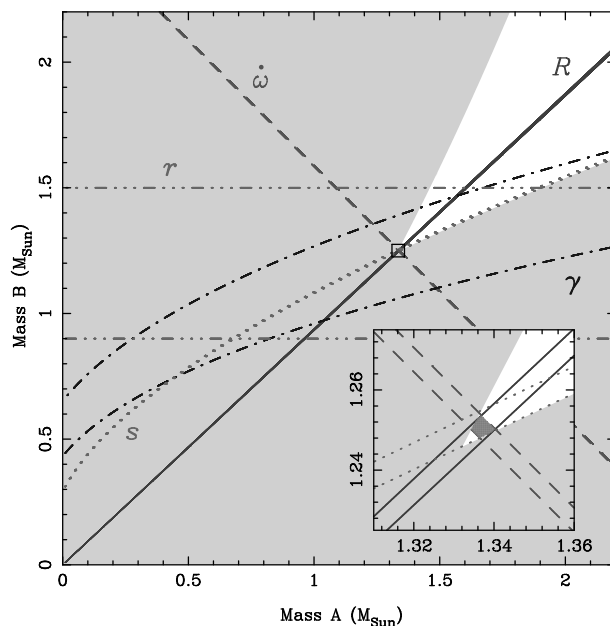


Figure 2. The observational constraints on the masses m_A and m_B . The solid regions are those which are excluded by the Keplerian mass functions of the two pulsars. Four further constraints are shown: (a) the measurement of the advance of periastron $\dot{\omega}$; (b) the measurement of $R = m_B/m_A$; (c) gravitational redshift parameter γ ; and (d) Shapiro delay parameters r and s . Insert: the intersection of the four constraints, with the scales increased by a factor of 50. The permitted regions are those between the pairs of parallel lines and the darker region is the only area permitted by all constraints.

rotational phase by the effect of gravitational deflection of the light in the field of the pulsar’s companion. This aberration-like effect would only be visible for very nearly edge-on systems, since it depends crucially on the orientation of the pulsar’s spin-axis in space. The double pulsar system fulfills these requirements.

Moment of Inertia In contrast to Newtonian physics, general relativity predicts that the neutron stars’ spins affect their orbital motion via spin-orbit coupling. This effect would be most clearly visible as a contribution to the observed $\dot{\omega}$ in a secular (Barker & O’Connell 1975), and periodic fashion (Wex 1995b). For the J0737–3039 system, the expected contribution is about an order of magnitude larger than for PSR B1913+16 (Lyne et al. 2004), i.e., $\sim 2 \times 10^{-4} \text{ deg yr}^{-1}$ (for A, assuming a geometry as determined for PSR B1913+16; see Kramer 1998). As the exact value depends on the pulsars’ moment of inertia, a measurement of this effect would allow the moment of inertia of a neutron star to be determined for the first time (Damour & Schäfer 1988). If two parameters, e.g., the Shapiro parameter s and the mass ratio R , can be measured sufficiently accurately, an

expected $\dot{\omega}_{\text{exp}}$ can be computed from the intersection point. This value can then be compared to the observed value $\dot{\omega}_{\text{obs}}$, which is given by (see Damour & Schäfer 1988)

$$\dot{\omega}_{\text{obs}} = \dot{\omega}_{\text{1PN}} \left[1 + \Delta\dot{\omega}_{\text{2PN}} - g^A \Delta\dot{\omega}_{\text{SO}}^A - g^B \Delta\dot{\omega}_{\text{SO}}^B \right], \quad (1)$$

where the last two terms represent contributions from the pulsars' spins. In these terms, $g^{A,B}$ are geometry-dependent factors, while $\Delta\dot{\omega}_{\text{SO}}^{A,B}$ arise from relativistic spin-orbit coupling (Barker & O'Connell 1975), formally at the first post-Newtonian (1PN) level. However, it turns out that, for binary pulsars, these effects have a magnitude comparable to second post-Newtonian (2PN) order (Wex 1995b), so that they only need to be considered if $\dot{\omega}$ is to be studied at this higher level of approximation. We find $\Delta\dot{\omega}_{\text{SO}} \propto I/Pm^2$ (Damour & Schäfer 1988), so that with precisely measured masses m the moment of inertia I can be measured and the neutron-star equation of state, as well as our understanding of matter at extreme pressures and densities, can be tested.

The dependence of $\Delta\dot{\omega}_{\text{SO}}$ on the spin period P suggests that only a measurement for pulsar A can be obtained. It also implies that at least two other parameters can be measured to a similar accuracy as $\dot{\omega}$. Despite being a tough challenge, e.g., due to the expected profile variation caused by geodetic precession, the prospects are promising. Simulations indicate that a few years of high-precision timing should be sufficient (Kramer et al., in preparation).

4. Conclusions

The double pulsar system provides not only improved but also completely new tests of general relativity. The current data indicate excellent agreement. For example, for the Shapiro parameter, $s_{\text{obs}}/s_{\text{exp}} = 1.0001 \pm 0.00220$ (Kramer et al., in preparation). The uncertainties are likely to decrease in the future, enabling the many other discussed applications.

Acknowledgments. MK thanks the Aspen Center for Physics and the organizers for financial support.

References

- Arzoumanian, Z. 1995, PhD thesis, Princeton University
- Barker, B. M., & O'Connell, R. F. 1975, *Phys. Rev. D*, 12, 329
- Börner, G., et al. 1975, *A&A*, 44, 417
- Burgay, M., et al. 2003, *Nature*, 426, 531
- Damour, T., & Deruelle, N. 1986, *Ann. Inst. H. Poincaré*, 44, 263
- Damour, T., Taylor, J. H. 1992, *Phys. Rev. D*, 45, 1840
- Damour, T., & Ruffini, R. 1974, *Acad. Sci. Paris Comptes Rendus, Ser. Sci. Math.*, 279
- Doroshenko, O. V., & Kopeikin, S. M. 1995, *MNRAS*, 274, 1029
- Kopeikin, S. M., & Schäfer, G. 1999, *Phys. Rev. D*, 60, 124002
- Kopeikin, S. 2003, in *Radio Pulsars*, ed. M. Bailes, D. Nice, & S. Thorsett (ASP Conf. Series), 111

- Kramer, M. 1998, *ApJ*, 509, 856
Lyne, A. G., et al. 2004, *Science*, 303, 1153
Weisberg, J. M., & Taylor, J. H. 2002, *ApJ*, 576, 942
Wex, N. 1995a, PhD thesis, Jena University, Jena, Germany
Wex, N. 1995b, *Class. Quantum Grav.*, 12, 983